Tableau Input Coupled Kinetic Equilibrium Transport (TICKET) Model

Supporting Information

Kevin J. Farley †,††*, Kevin J. Rader ‡, and Benjamin E. Miller ‡‡

† Civil and Environmental Engineering, Manhattan College, Riverdale, NY 10471

†† HydroQual, Inc. Mahwah, NJ 07430

‡ Civil and Environmental Engineering, University of Delaware, Newark, DE 19716

‡‡ Civil and Environmental Engineering, University of Massachusetts Lowell, Lowell, MA 01854

Number of Pages: 19

Number of Figures: 5

Number of Tables: 4

*Corresponding author. Tel.: (718) 862-7383, fax: (718) 862-8035
E-mail: kevin.farley@manhattan.edu

Verification Studies

(a) Subsurface Transport of Major Cations

An experimental field study was conducted by Valocchi et al. (1) to examine the transport of cations (Mg^{2+}, Ca^{2+} and Na^{+}) through a subsurface aquifer. In the study, treated municipal wastewater was continuously injected into the aquifer and groundwater was monitored at a sampling well 16 meters away from the injection point. Studies by Valocchi et al. (1) revealed the dominant processes affecting breakthrough of Mg^{2+}, Ca^{2+} and Na^{+} at the sampling well were advection, dispersion, and equilibrium heterovalent ion exchange. This problem was chosen as a test case because it is chemically simple, involves real field data, and has been used as a test problem in several other modeling studies (2-6).

The problem was modeled in one-dimension by assuming radially symmetric flow and using sixteen cells to represent concentric annuli of the aquifer around the injection point. The aquifer thickness, porosity and bulk density were 2.0 m, 0.25 and 1.875 kg / L, respectively. The time step was set at 1 hour for numerical integration and the total simulation time was 5,000 hours. The transport through the aquifer was fitted to the breakthrough curve for a chloride tracer injection using a flow rate of 26.5 m^3 / hr and a dispersivity of 1 m. (The flow rate of 26.5 m^3 / hr is slightly higher than the reported injection rate of 21 m^3 / hr and reflects aquifer heterogeneity with a higher permeability in the direction of the monitoring well.)

The input tableau for equilibrium ion exchange reactions is given in Table S1. Note that equilibrium ion exchange constants for Mg^{2+} and Ca^{2+} were obtained from independent batch equilibrium experiments (1). Concentrations of Cl^{-}, Na^{+}, Mg^{2+}, and Ca^{2+} in the injection water were 9.027, 9.395, 0.494, and 2.121 mM, respectively. Average dissolved concentrations of Cl^{-}, Na^{+}, Mg^{2+}, and Ca^{2+} in the "native" groundwater were 125.5, 69.38, 15.35, and 8.807 mM and

the corresponding initial concentrations of $TotCl^-$, $TotMg^{2+}$, $TotCa^{2+}$, $TotNa^+$ and TotNaX concentrations were determined to be 125.5, 161, 156, -517, and 750 mM based on an initial speciation calculation.

TICKET-calculated and measured concentrations of Mg^{2+} and Ca^{2+} at the monitoring well are presented in Figure S1 as a function of the injected volume of wastewater. As shown, the model results provide a good description of observed Mg^{2+} concentrations and show an initial flushing of the high Mg^{2+} groundwater. This is followed by a second front of Mg^{2+} as Ca^{2+} (with the higher selectivity coefficient) displaces the bound Mg^{2+}. Final concentrations of Mg^{2+} and Ca^{2+} at the monitoring well approach the injected Mg^{2+} and Ca^{2+} concentrations at the end of the simulation period. The TICKET results shown in Figure S1 were also found to be consistent with results from the other model studies listed above. This case provides a good first test of the utility of TICKET in modeling a classical, albeit a simple, chemical equilibrium and subsurface transport problem.

(b) Fe(II)-As(III) Batch Oxidation Study

There is currently a growing interest in understanding the role of various free radicals in the oxidation of metals and metalloids. For example, the effect of iron redox chemistry on the oxidation of As(III) in oxic systems through the formation of various free radicals has recently been examined by Hug and Leupin (7). A depiction of their proposed mechanism for Fe(II)-catalyzed oxidation of As(III) is given in Figure 2 of the paper. Briefly, the sequence begins with a series of one-electron transfers in which molecular oxygen is reduced to superoxide and hydrogen peroxide as Fe(II) is oxidized to Fe(III). The subsequent reaction of Fe(II) with hydrogen peroxide produces the intermediates INT and INT-OH, respectively. These two

species interconvert rapidly enough such that they are considered to be in equilibrium. Each of the two intermediates produces a different species capable of oxidizing arsenic. At low pH (< 5.24), where equilibrium favors INT, the hydroxyl radical is formed along with Fe(III). At high pH (> 5.24), where equilibrium favors INT-OH, an Fe(IV) species is formed. For this latter case (pH > 5.24), another sequence of one-electron transfers follows the formation of the Fe(IV) species. As(III) is oxidized to As(IV) as Fe(IV) is reduced to Fe(III), and then As(IV) is oxidized to As(V) as molecular oxygen is reduced to superoxide. Alternatively, the Fe(IV) produced from INT-OH can also be reduced by Fe(II) to form Fe(III) as Fe(II) is oxidized to Fe(III). This competitive pathway for Fe(IV) reaction with Fe(II) is important in ultimately controlling the extent of As(III) oxidation.

Based on laboratory and model studies, Hug and Leupin (7) developed a detailed description of the Fe(II)-catalyzed As(III) oxidation sequence. For this purpose, modeling calculations were performed using ACUCHEM (8), a computer program for modeling complex kinetic reactions in batch systems. A full list of reactions, along with chemical equilibrium constants and kinetic rate coefficients, is given in Hug and Leupin (7).

Comparative simulations were performed with ACUCHEM and TICKET to provide a rigorous test of TICKET's ability to model complex reaction sequences with equilibrium, fast kinetics and transient intermediate species in a batch system. The time step was set at 0.00001 minutes for TICKET with a total simulation time of 2 minutes. The TICKET input tableau for this simulation is given in Table S2, and the corresponding results for the ACUCHEM and TICKET simulations are presented in Figure S2 for an initial concentrations of 1,380 μM Fe(II) and 138 μM As(III), and a fixed dissolved oxygen concentration and pH of 250 μM and 8.0,

respectively.

As shown in Figure S2, TICKET-calculated results are indistinguishable from ACUCHEM. At the beginning of the simulation, Fe(II) is oxidized producing low concentrations of the intermediate, Fe(IV). The Fe(IV) is then utilized in oxidizing As(III) to the intermediate As(IV) which is subsequently oxidized to As(V). Because Fe(IV) is also being consumed in a competitive reactions with Fe(II), only 15% of the As(III) is oxidized in the batch system simulation.

(c) Calcite and Dolomite Precipitation in a Packed Column

This problem, along with corresponding model results, is described in the paper. The input tableau for the problem is given in Table S3

Application Studies

Fe(II)-Catalyzed As(III) Oxidation Column Study

This problem is described in the paper. For model simulations, the column cross-sectional area was taken as 63.6 cm^2, the overlying water was considered to be a well-mixed cell of 6.3 cm, and the underlying sediment of 10 cm was divided into 20 – 0.5 cm layers. The porosity of the sediment was taken as 0.38 and transport in the column was assumed to occur solely through diffusion. For simplicity, a single diffusion coefficient of 1.0 cm^2 day^{-1} was specified for all dissolved species. Pore water was initially anoxic with total Fe(II) and As(III) concentrations of 1,790 μM and 179 μM, respectively, and pH was fixed at 8.3 throughout the column.. The TICKET input tableau is given in Table S4. The time step was set equal to 0.005 days for all simulations presented in the paper.

Metal Cycling in an Idealized Lake

TICKET model simulations were performed to examine the cycling of metals in an idealized lake with a well-mixed water column and an underlying sediment layer. For this purpose, transport in the lake is described by the inflow and outflow of dissolved and particulate chemical, settling, resuspension and burial of particulate chemical, and diffusive exchange of dissolved chemical across the water-sediment interface (Figure S3). Chemical speciation calculations for the water column and sediment layer are based on metal complexation to inorganic ligands $\left(OH^-, CO_3^{2-}, HCO_3^-, SO_4^{2-}, Cl^-\right)$, and to dissolved (DOC) and particulate organic carbon (POM) using electrostatic corrections and binding constants from the Windermere Humic Acid Model, WHAM V (11). In addition, precipitation of metal sulfides in sediment is also considered (12).

For model simulations, a circumneutral pH (pH=7), soft water lake (hardness = 50 mg as $CaCO_3$/L) was considered. The surface area, average depth and hydraulic residence time of the lake are given as 10 km^2, 10 m, and 1 year, respectively. Settling velocity, burial rate and diffusive exchange rate are specified as 60 m/yr, 0.2 cm/yr, and 1 cm/day, and resuspension was considered to be negligible. Water column DOM and POM concentrations were taken as 6 mg/L and 2 mg/L, respectively, and are representative of a moderately productive lake. Sediment solids concentration, fraction organic matter, DOM, and sulfide concentrations were taken as 400 g solids/L, 0.05, 6 mg/L, and 20 μmole sulfide/g solids, respectively. Based on these values, the average annual organic carbon and sulfide cycles in the lake are described by net production and consumption rates (Figure S4). See Farley et al. (13) for further details.

Steady-state model results for Cu and Cd are shown in Figure S5. For Cu (Figure S5a),

which has a strong affinity to bind to organic matter, a large amount of Cu in the water column is bound to POM. This results in a large settling flux of Cu to the sediment. As organic matter diagenesis occurs in the sediment, Cu is released from the settled POM. A portion of the released Cu is precipitated as CuS(s) or concentrated on the remaining POM, and ultimately buried in the deeper sediment. The remainder of the released Cu accumulates in the pore water, resulting in higher Cu activity in the pore water (than the overlying water) and a diffusive flux of Cu back to the water column.

Cu results are in contrast to results for Cd, which has a much weaker affinity to bind to organic matter. As shown (Figure S5b), Cd binding to POM is greatly reduced and most of the Cd is present in the overlying water as free metal. A large fraction of the Cd is therefore removed from the lake in the outflow, and a smaller fraction of Cd is removed from the water column by settling. In contrast to Cu, the settling flux of Cd to the sediment is less than the sulfide production rate, and virtually all of the Cd in sediment precipitates as CdS(s). This results in a much lower activity of free Cd in the pore water and induces the diffusion of dissolved Cd from the overlying water to the sediment. This additional input of Cd to the sediment also precipitates as CdS(s) and is ultimately buried in the deeper sediment. These results demonstrate the importance of metal binding affinity to organic matter in assessing metal cycling in lakes. Other parameters (such as pH, hardness, organic matter and sulfur cycling, flow rates, settling, burial, etc.) will also play a critical roles in determining metal cycling and exposure (13).

References

1. Valocchi, A.J.; Street, R.L.; Roberts, P.V. Transport of ion-exchanging solutes in groundwater: chromatographic theory and field simulation. *Water Resour. Res.* **1981**, *17*, 1517-1527.

2. Miller, C.W.; Benson, L.V. Simulation of solute transport in a chemically reactive heterogeneous system. *Water Resour. Res*. **1983**, *19*, 381-391.

3. Cederberg, G.A.; Street, R.L.; Leckie, J.O. Groundwater mass transport and equilibrium chemistry model for multicomponent systems. *Water Resour. Res*. **1985**, *21*, 1095-1104.

4. Van Ommen, H.C. 'Mixing-cell' concept applied to transport of non-reactive and reactive components in soils and groundwater. *J. Hydrol*. **1985**, *78*, 201-213.

5. Charbeneau, R.J. Multicomponent exchange and subsurface solute transport: characteristics, coherence, and the Riemann problem. *Water Resour. Res*. **1988**, *24*, 57-64.

6. Appelo, C.A.J. Some calculations on multicomponent transport with cation exchange in aquifers. *Ground Water*, **1994**, *32*, 968-975.

7. Hug, S.J. and Leupin, O. Iron-catalyzed oxidation of arsenic(III) by oxygen and by hydrogen peroxide: pH-dependent formation of oxidants in the Fenton reaction. *Environ. Sci. Technol*., **2003**, *37*, 2734-2742.

8. Braun, W.; Herron, J.T.; Kahaner, D.K. Acuchem: Computer program for modeling complex chemical reaction systems. *Int. J. Chem. Kinet.* **1988**, *20*, 51-62.

9. Engesgaard, P.; Kipp, K.L. Geochemical transport model for redox-controlled movement of mineral fronts in groundwater flow systems: a case of nitrate removal by oxidation of pyrite. *Water Resour. Res*. **1992**, *28*, 2829-2843.

10. Bisceglia, K.J.; Rader, K.J.; Carbonaro, R.F.; Farley, K.J.; Mahony, J.D.; Di Toro, D.M. Iron(II)-catalyzed oxidation of arsenic(III) in a sediment column. *Environ. Sci. Technol*., **2005**, *39*, 9217-9222.

11. Tipping, E. WHAM—a chemical equilibrium model and computer code for waters, sediments, and soils incorporating a discrete site/electrostatic model of ion-binding by humic substances. *Comput. Geosci*. **1994**, 20, 973 - 1023.

12. Di Toro, D.M.; Mahony, J.D.; Hansen, D.J.; Scott, K.J.; Carlson, A.R.; Ankley, G.T. Acid volatile sulfide predicts the acute toxicity of cadmium and nickel in sediments. *Environ.*

Sci.Technol., **1992**, *26*, 96-101.

13. Farley, K.J.; Carbonaro, R.F.; Di Toro, D.M. “Unit World Model: Tier 1 Model for Metals in Lakes.” Report to International Council of Mining and Metals (ICMM) and Eurometaux, 30 p, 2005.

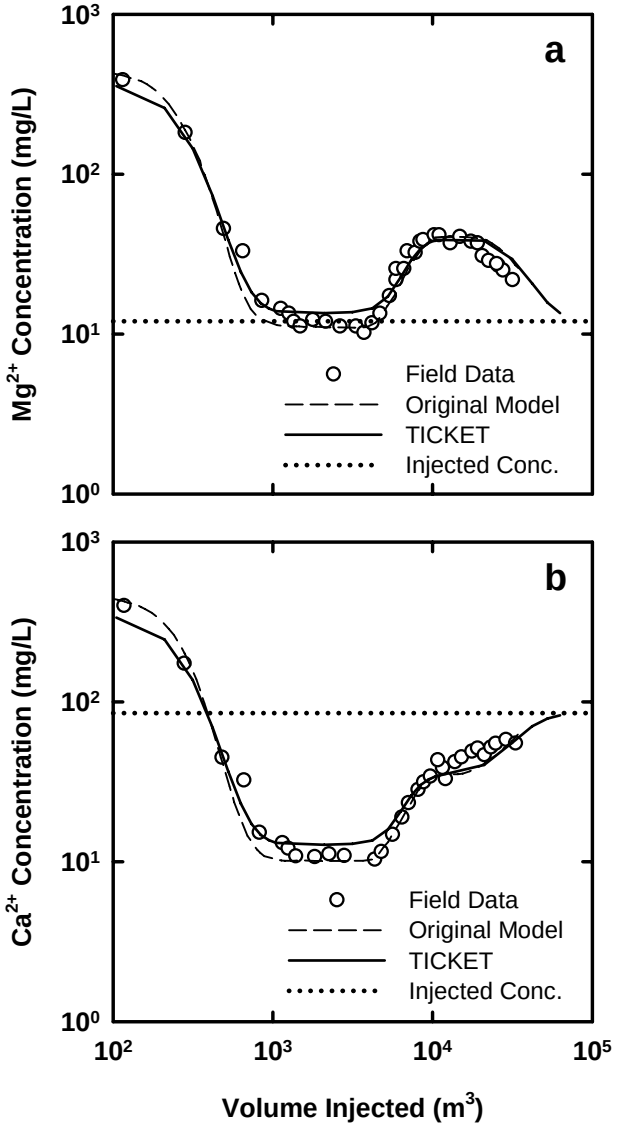

Figure S1. Comparison of TICKET-calculated breakthrough curve for (a) Mg^{2+} and (b) Ca^{2+} with field data and model results of Valocchi et al. (1).

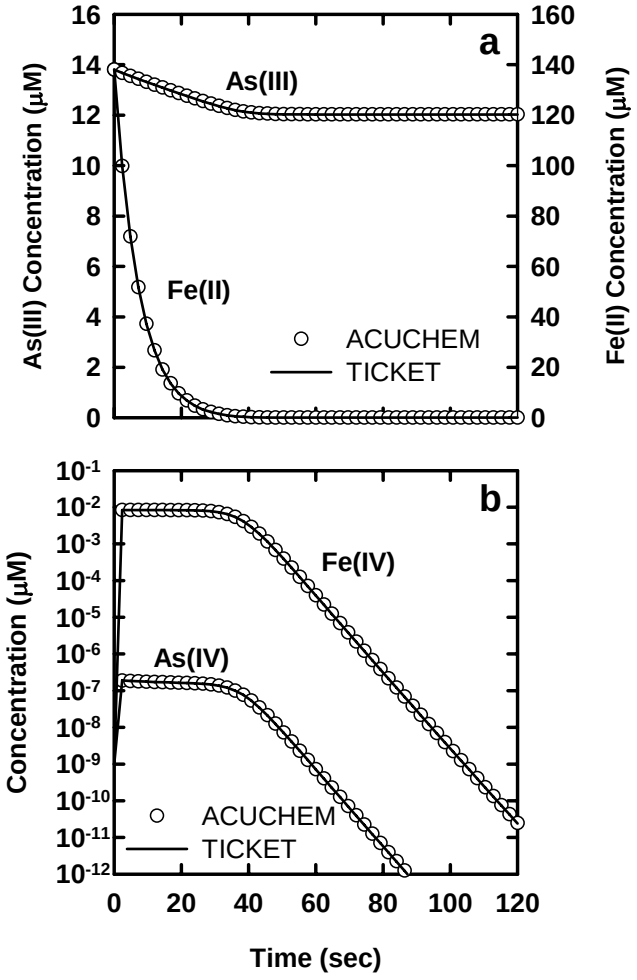

Figure S2. Comparison of TICKET and ACUCHEM (8) model results for Fe(II)-catalyzed oxidation of As(III) in batch systems at fixed dissolved oxygen concentration and pH of 250 μM and 8.0, respectively.

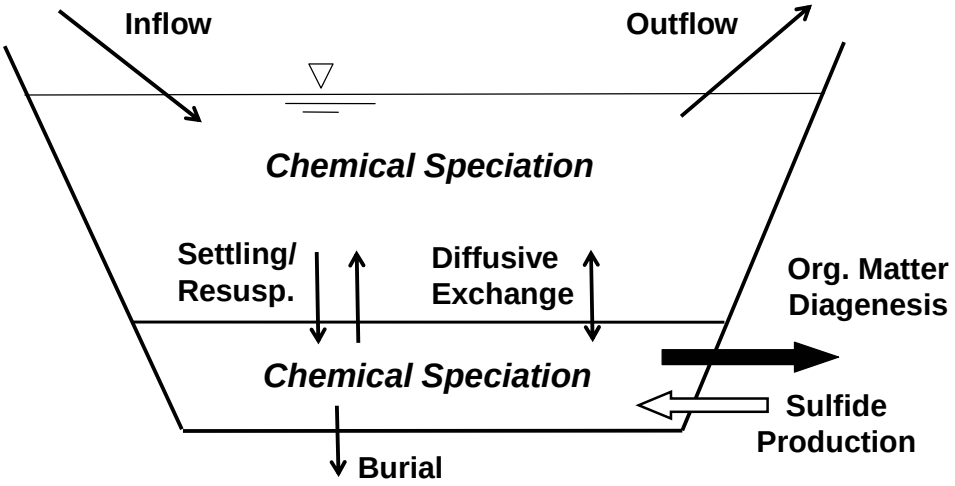

Figure S3. Modeling framework for metal cycling in an idealized lake.

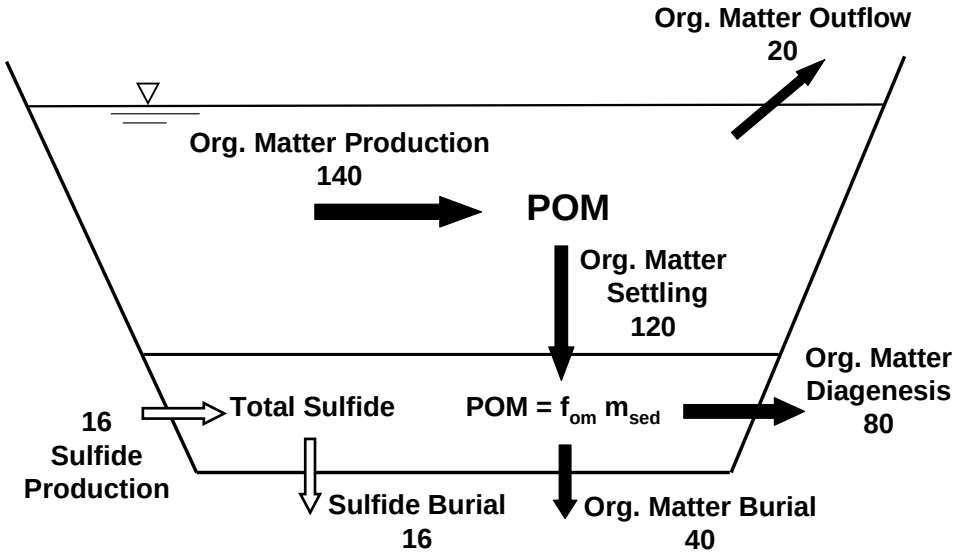

Figure S4. Average annual organic matter and sulfide cycles in lake.

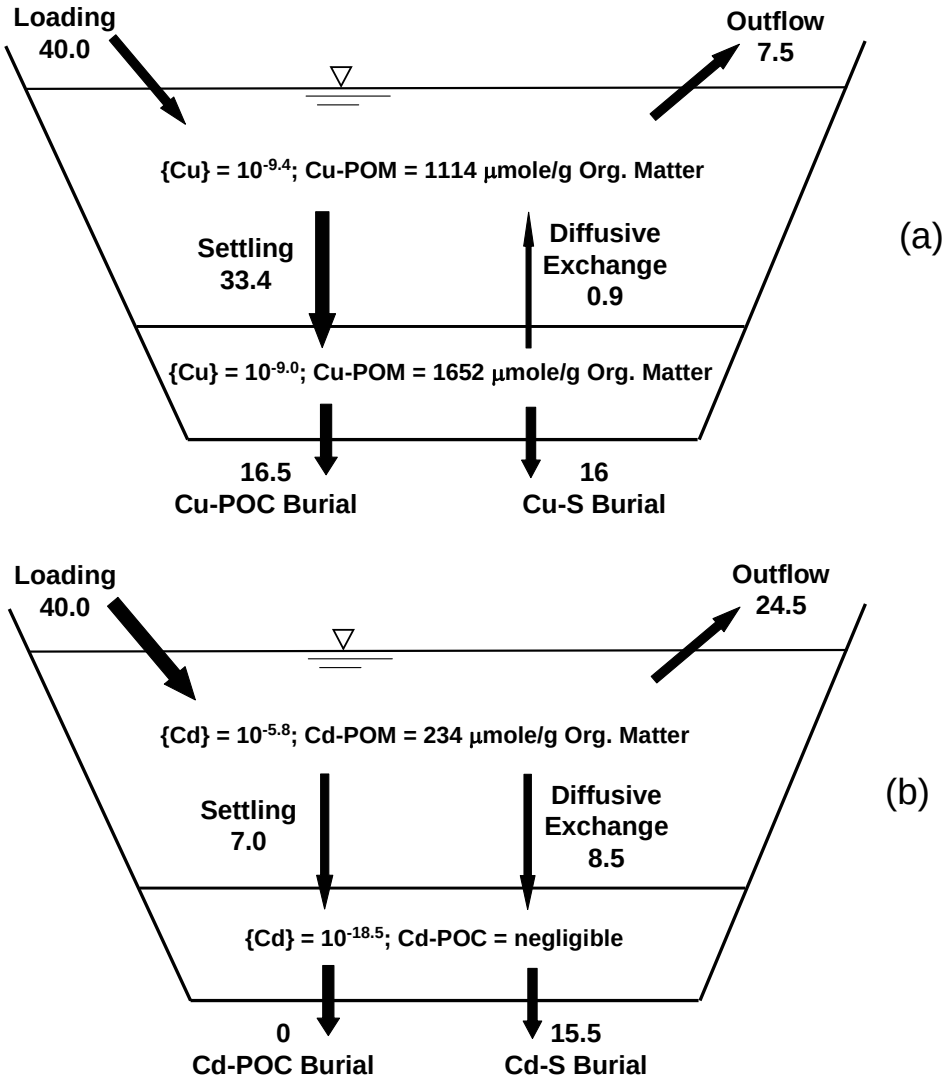

Figure S5. Steady-state concentrations and fluxes for copper (a) and (b) cadmium in a circumneutral, soft water lake. (Metal flux rates, as depicted by arrows on the diagrams above, are given in mmoles / m^2 / yr.)

Table S1. TICKET Input Tableau for Subsurface Transport of Major Cations

	Mg^{2+}	Ca^{2+}	Na^{+}	NaX		Mq	Me	Mw
Species					log K			
Mg^{2+}	1,1				0	1	1	0
Ca^{2+}		1,1			0	1	1	0
Na^{+}			1,1		0	1	1	0
NaX				1,1	0	0	0	0
MgX_2	1,1		-2,-2	2,2	0.35	0	0	0
CaX_2		1,1	-2,-2	2,2	0.60	0	0	0
Kinetic Reactions					k			

Notes:

(a) X represents the ion exchange sites on the aquifer material.

(b) The selectivity coefficients of Valocchi et al. (1) were divided by the bulk density (1875 g/L) and the ion exchange capacity (10^{-4} eq/g) to convert to equilibrium coefficients on a mole/L basis.

(c) The injected water was specified as: 320 mg/L (9.027 mM) of Cl^{-}, 216 mg/L (9.395 mM) of Na^{+}, 12 mg/L (0.494 mM) of Mg^{2+}, and 85 mg/L (2.121 mM) of Ca^{2+}

(d) The native water was specified as average concentrations of: 4450 mg/L (125.5 mM) of Cl^{-}, 1573 mg/L (69.38 mM) of Na^{+}, 373 mg/L (15.35 mM) of Mg^{2+}, and 353 mg/L (8.807 mM) of Ca^{2+}

(e) Initial speciation calculations were performed using the native pore water concentrations and the selectivity coefficients to determine the total (pore water + bound) chemical concentrations. From this calculation, $TotCl^{-}$, $TotMg^{2+}$, $TotCa^{2+}$, $TotNa^{+}$ and TotNaX concentrations were determined to be 125.5, 161, 156, -517, and 750 mM.

Table S2. TICKET Input Tableau for Fe-Catalyzed Oxidation of As(III) for a Batch System after Hug and Leupin (7)

	As(III)	As(IV)	As(V)	Fe^{2+}	Fe^{3+}	precip	iprecip	Fe(IV)	O_2	O_2*-	H_2O_2	INT-OH	H_2CO_3	*OH	CO_3*-	$FeCO_3^+$	INT-CO_3	
Species																		log K
As(III)	1,1	0,0	0,0	0,0	0,0	0,0	0,0	0,0	0,0	0,0	0,0	0,0	0,0	0,0	0,0	0,0	0,0	0
As(IV)	0,0	1,1	0,0	0,0	0,0	0,0	0,0	0,0	0,0	0,0	0,0	0,0	0,0	0,0	0,0	0,0	0,0	0
As(V)	0,0	0,0	1,1	0,0	0,0	0,0	0,0	0,0	0,0	0,0	0,0	0,0	0,0	0,0	0,0	0,0	0,0	0
Fe^{2+}	0,0	0,0	0,0	1,1	0,0	0,0	0,0	0,0	0,0	0,0	0,0	0,0	0,0	0,0	0,0	0,0	0,0	0
Fe^{3+}	0,0	0,0	0,0	0,0	1,1	0,0	0,0	0,0	0,0	0,0	0,0	0,0	0,0	0,0	0,0	0,0	0,0	0
precip	0,0	0,0	0,0	0,0	0,0	1,1	0,0	0,0	0,0	0,0	0,0	0,0	0,0	0,0	0,0	0,0	0,0	0
iprecip	0,0	0,0	0,0	0,0	0,0	0,0	1,1	0,0	0,0	0,0	0,0	0,0	0,0	0,0	0,0	0,0	0,0	0
Fe(IV)	0,0	0,0	0,0	0,0	0,0	0,0	0,0	1,1	0,0	0,0	0,0	0,0	0,0	0,0	0,0	0,0	0,0	0
O_2	0,0	0,0	0,0	0,0	0,0	0,0	0,0	0,0	1,1	0,0	0,0	0,0	0,0	0,0	0,0	0,0	0,0	0
O_2*-	0,0	0,0	0,0	0,0	0,0	0,0	0,0	0,0	0,0	1,1	0,0	0,0	0,0	0,0	0,0	0,0	0,0	0
H_2O_2	0,0	0,0	0,0	0,0	0,0	0,0	0,0	0,0	0,0	0,0	1,1	0,0	0,0	0,0	0,0	0,0	0,0	0
INT-OH	0,0	0,0	0,0	0,0	0,0	0,0	0,0	0,0	0,0	0,0	0,0	1,1	0,0	0,0	0,0	0,0	0,0	0
H_2CO_3	0,0	0,0	0,0	0,0	0,0	0,0	0,0	0,0	0,0	0,0	0,0	0,0	1,1	0,0	0,0	0,0	0,0	0
*OH	0,0	0,0	0,0	0,0	0,0	0,0	0,0	0,0	0,0	0,0	0,0	0,0	0,0	1,1	0,0	0,0	0,0	0
CO_3*-	0,0	0,0	0,0	0,0	0,0	0,0	0,0	0,0	0,0	0,0	0,0	0,0	0,0	0,0	1,1	0,0	0,0	0
$FeCO_3^+$	0,0	0,0	0,0	0,0	0,0	0,0	0,0	0,0	0,0	0,0	0,0	0,0	0,0	0,0	0,0	1,1	0,0	0
INT-CO_3	0,0	0,0	0,0	0,0	0,0	0,0	0,0	0,0	0,0	0,0	0,0	0,0	0,0	0,0	0,0	0,0	1,1	0
Sand	0,0	0,0	0,0	0,0	0,0	0,0	0,0	0,0	0,0	0,0	0,0	0,0	0,0	0,0	0,0	0,0	0,0	0
$FeOH^+$	0,0	0,0	0,0	1,1	0,0	0,0	0,0	0,0	0,0	0,0	0,0	0,0	0,0	0,0	0,0	0,0	0,0	-1.51
$FeCO_3$	0,0	0,0	0,0	1,1	0,0	0,0	0,0	0,0	0,0	0,0	0,0	0,0	1,1	0,0	0,0	0,0	0,0	5.01
$FeOH_2^+$	0,0	0,0	0,0	0,0	1,1	0,0	0,0	0,0	0,0	0,0	0,0	0,0	0,0	0,0	0,0	0,0	0,0	5.7
$Fe(OH)_2^+$	0,0	0,0	0,0	0,0	1,1	0,0	0,0	0,0	0,0	0,0	0,0	0,0	0,0	0,0	0,0	0,0	0,0	10.1
$Fe(OH)_3$	0,0	0,0	0,0	0,0	1,1	0,0	0,0	0,0	0,0	0,0	0,0	0,0	0,0	0,0	0,0	0,0	0,0	10.2
HO_2	0,0	0,0	0,0	0,0	0,0	0,0	0,0	0,0	0,0	1,1	0,0	0,0	0,0	0,0	0,0	0,0	0,0	-3.2
INT	0,0	0,0	0,0	0,0	0,0	0,0	0,0	0,0	0,0	0,0	0,0	1,1	0,0	0,0	0,0	0,0	0,0	-2.76
HCO_3^-	0,0	0,0	0,0	0,0	0,0	0,0	0,0	0,0	0,0	0,0	0,0	0,0	1,1	0,0	0,0	0,0	0,0	1.65
CO_3^{2-}	0,0	0,0	0,0	0,0	0,0	0,0	0,0	0,0	0,0	0,0	0,0	0,0	1,1	0,0	0,0	0,0	0,0	-0.68

Table S2 (continued). TICKET Input Tableau for Fe-Catalyzed Oxidation of As(III) for a Batch System after Hug and Leupin (7)

Kinetic Reactions	As(III)	As(IV)	As(V)	Fe^{2+}	Fe^{3+}	precip	iprecip	Fe(IV)	O_2	O_2*-	H_2O_2	INT-OH	H_2CO_3	*OH	CO_3*-	$FeCO_3^+$	INT-CO_3	k
A1	1,-1	0,1	0,0	0,0	0,0	0,0	0,0	0,0	0,0	0,0	0,0	0,0	0,0	1,-1	0,0	0,0	0,0	4.80E+11
A2	1,-1	0,1	0,0	0,0	0,0	0,0	0,0	0,0	0,0	0,0	0,0	0,0	0,1	0,0	1,-1	0,0	0,0	6.60E+09
A3	0,0	1,-1	0,1	0,0	0,0	0,0	0,0	0,0	1,-1	0,1	0,0	0,0	0,0	0,0	0,0	0,0	0,0	6.60E+10
B1	0,0	0,0	0,0	1,-1	0,1	0,0	0,0	0,0	1,-1	0,1	0,0	0,0	0,0	0,0	0,0	0,0	0,0	8.40E+03
B2	0,0	0,0	0,0	1,-1	0,1	0,0	0,0	0,0	0,0	1,-1	0,1	0,0	0,0	0,0	0,0	0,0	0,0	6.00E+08
B3	0,0	0,0	0,0	1,-1	0,1	0,0	0,0	0,0	0,0	1,-1	0,1	0,0	0,0	0,0	0,0	0,0	0,0	4.54E+04
B4	0,0	0,0	0,0	1,-1	0,1	0,0	0,0	0,0	0,0	0,0	0,0	0,0	0,0	1,-1	0,0	0,0	0,0	1.92E+10
B5	0,0	0,0	0,0	1,-1	0,1	0,0	0,0	0,0	0,0	0,0	0,0	0,0	0,1	0,0	1,-1	0,0	0,0	2.16E+10
F1	0,0	0,0	0,0	1,-1	0,0	0,0	0,0	0,0	0,0	0,0	1,-1	0,1	0,0	0,0	0,0	0,0	0,0	1.61E+03
F2	0,0	0,0	0,0	1,-1	0,0	0,0	0,0	0,0	0,0	0,0	1,-1	0,1	0,0	0,0	0,0	0,0	0,0	2.44E+07
F3	0,0	0,0	0,0	1,-1	0,0	0,0	0,0	0,0	0,0	0,0	1,-1	0,0	1,-1	0,0	0,0	0,0	0,1	5.35E+12
I2	0,0	0,0	0,0	0,0	0,1	0,0	0,0	0,0	0,0	0,0	0,0	1,-1	0,0	0,1	0,0	0,0	0,0	1.04E+05
I3	0,0	0,0	0,0	0,0	0,0	0,0	0,0	0,1	0,0	0,0	0,0	1,-1	0,0	0,0	0,0	0,0	0,0	6.00E+07
I4	0,0	0,0	0,0	0,0	0,1	0,0	0,0	0,0	0,0	0,0	0,0	0,0	0,0	0,0	0,1	0,0	1,-1	6.00E+07
I5	0,0	0,0	0,0	0,0	0,0	0,0	0,0	0,1	0,0	0,0	0,0	0,0	0,1	0,0	0,0	0,0	1,-1	2.56E+08
J1	0,0	0,0	0,0	1,-1	0,2	0,0	0,0	1,-1	0,0	0,0	0,0	0,0	0,0	0,0	0,0	0,0	0,0	1.14E+05
J2	0,0	0,0	0,0	1,-1	0,2	0,0	0,0	1,-1	0,0	0,0	0,0	0,0	0,0	0,0	0,0	0,0	0,0	2.50E+08
J3	0,0	0,0	0,0	1,-1	0,1	0,0	0,0	1,-1	0,0	0,0	0,0	0,0	1,-1	0,0	0,0	0,1	0,0	2.23E+13
J4	1,-1	0,1	0,0	0,0	0,1	0,0	0,0	1,-1	0,0	0,0	0,0	0,0	0,0	0,0	0,0	0,0	0,0	2.50E+07
J5	0,0	0,0	0,0	0,0	0,1	0,0	0,0	0,0	0,0	0,0	0,0	0,0	0,1	0,0	0,0	1,-1	0,0	6.00E+10
R1	0,0	0,0	0,0	0,1	1,-1	0,0	0,0	0,0	0,1	1,-1	0,0	0,0	0,0	0,0	0,0	0,0	0,0	9.00E+09
R2	0,0	0,0	0,0	0,1	1,-1	0,0	0,0	0,0	0,1	1,-1	0,0	0,0	0,0	0,0	0,0	0,0	0,0	4.51E+15
R3	0,0	0,0	0,0	0,1	1,-1	0,0	0,0	0,0	0,1	1,-1	0,0	0,0	0,0	0,0	0,0	0,0	0,0	1.13E+20
O1	0,0	0,0	0,0	0,0	0,0	0,0	0,0	0,0	0,0	2,-2	0,1	0,0	0,0	0,0	0,0	0,0	0,0	3.67E+06
O2	0,0	0,0	0,0	0,0	0,0	0,0	0,0	0,0	0,0	2,-2	0,1	0,0	0,0	0,0	0,0	0,0	0,0	1.98E+01
O3	0,0	0,0	0,0	0,0	0,0	0,0	0,0	0,0	0,0	0,1	1,-1	0,0	0,0	1,-1	0,0	0,0	0,0	1.80E+09
O4	0,0	0,0	0,0	0,0	0,0	0,0	0,0	0,0	0,0	0,0	0,0	0,0	1,-1	1,-1	0,1	0,0	0,0	2.28E+10
O5	0,0	0,0	0,0	0,0	0,0	0,0	0,0	0,0	0,0	0,1	1,-1	0,0	0,1	0,0	1,-1	0,0	0,0	2.58E+07
P1	0,0	0,0	0,0	0,0	2,-2	0,1	0,1	0,0	0,0	0,0	0,0	0,0	0,0	0,0	0,0	0,0	0,0	2.94E+30
P2	0,0	0,0	0,0	0,0	1,-1	1,0	0,1	0,0	0,0	0,0	0,0	0,0	0,0	0,0	0,0	0,0	0,0	1.85E+20

Note:

(a) All kinetic reaction rates (k) are given in M^{-1} $minutes^{-1}$ or $minutes^{-1}$

(b) Reactions are identifed in Hug and Leupin (2003)

(c) Reaction rate coefficients are specified at pH = 8.0

Table S3. TICKET Input Tableau for Calcite Dissolution / Dolomite Precipitation in a Packed Column after Engesgaard and Kipp (9)

	Cl^-	H^+	Ca^{2+}	Mg^{2+}	CO_3^{2-}	S_calcite	TS_calcite	S_dolomite	TS_dolomite	
Species										log K
Cl^-	1,1	0,0	0,0	0,0	0,0	0,0	0,0	0,0	0,0	0
H^+	0,0	1,1	0,0	0,0	0,0	0,0	0,0	0,0	0,0	0
Ca^{2+}	0,0	0,0	1,1	0,0	0,0	0,0	0,0	0,0	0,0	0
Mg^{2+}	0,0	0,0	0,0	1,1	0,0	0,0	0,0	0,0	0,0	0
CO_3^{2-}	0,0	0,0	0,0	0,0	1,1	0,0	0,0	0,0	0,0	0
OH^-	0,0	-1,1	0,0	0,0	0,0	0,0	0,0	0,0	0,0	-14.01
HCO_3^-	0,0	1,1	0,0	0,0	1,1	0,0	0,0	0,0	0,0	10.31
H_2CO_3	0,0	2,2	0,0	0,0	1,1	0,0	0,0	0,0	0,0	16.71
$CaCO_3$ (aq)	0,0	0,0	1,1	0,0	1,1	0,0	0,0	0,0	0,0	3.23
$MgCO_3$ (aq)	0,0	0,0	0,0	1,1	1,1	0,0	0,0	0,0	0,0	2.98
Calcite(s)	0,0	0,0	1,1	0,0	1,1	0,0	1,0	0,0	0,0	8.47
{Calcite(s)}	0,0	0,0	1,0	0,0	1,0	0,0	0,1	0,0	0,0	8.47
S_calcite(s)	0,0	0,0	0,0	0,0	0,0	1,1	1,0	0,0	0,0	0
{S_calcite(s)}	0,0	0,0	0,0	0,0	0,0	1,0	0,1	0,0	0,0	0
Dolomite(s)	0,0	0,0	1,1	1,1	2,2	0,0	0,0	0,0	1,0	17.17
{Dolomite(s)}	0,0	0,0	1,0	1,0	2,0	0,0	0,0	0,0	0,1	17.17
S_dolomite(s)	0,0	0,0	0,0	0,0	0,0	0,0	0,0	1,1	1,0	0
{S_dolomite(s)}	0,0	0,0	0,0	0,0	0,0	0,0	0,0	1,0	0,1	0
Kinetic Reactions										k

Table S4. TICKET Input Tableau for Fe-Catalyzed Oxidation of As(III) in the Sediment Column.
Based on information from Bisceglia et al. (10)

	As(III)	As(IV)	As(V)	Fe^{2+}	Fe^{3+}	precip	iprecip	Fe(IV)	O_2	O_2*-	H_2O_2	INT-OH	Sand	
Species														log K
As(III)	1,1	0,0	0,0	0,0	0,0	0,0	0,0	0,0	0,0	0,0	0,0	0,0	0,0	0
As(IV)	0,0	1,1	0,0	0,0	0,0	0,0	0,0	0,0	0,0	0,0	0,0	0,0	0,0	0
As(V)	0,0	0,0	1,1	0,0	0,0	0,0	0,0	0,0	0,0	0,0	0,0	0,0	0,0	0
Fe^{2+}	0,0	0,0	0,0	1,1	0,0	0,0	0,0	0,0	0,0	0,0	0,0	0,0	0,0	0
Fe^{3+}	0,0	0,0	0,0	0,0	1,1	0,0	0,0	0,0	0,0	0,0	0,0	0,0	0,0	0
precip	0,0	0,0	0,0	0,0	0,0	1,1	0,0	0,0	0,0	0,0	0,0	0,0	0,0	0
iprecip	0,0	0,0	0,0	0,0	0,0	0,0	1,1	0,0	0,0	0,0	0,0	0,0	0,0	0
Fe(IV)	0,0	0,0	0,0	0,0	0,0	0,0	0,0	1,1	0,0	0,0	0,0	0,0	0,0	0
O_2	0,0	0,0	0,0	0,0	0,0	0,0	0,0	0,0	1,1	0,0	0,0	0,0	0,0	0
O_2*-	0,0	0,0	0,0	0,0	0,0	0,0	0,0	0,0	0,0	1,1	0,0	0,0	0,0	0
H_2O_2	0,0	0,0	0,0	0,0	0,0	0,0	0,0	0,0	0,0	0,0	1,1	0,0	0,0	0
INT-OH	0,0	0,0	0,0	0,0	0,0	0,0	0,0	0,0	0,0	0,0	0,0	1,1	0,0	0
Sand	0,0	0,0	0,0	0,0	0,0	0,0	0,0	0,0	0,0	0,0	0,0	0,0	1,1	0
$FeOH^+$	0,0	0,0	0,0	1,1	0,0	0,0	0,0	0,0	0,0	0,0	0,0	0,0	0,0	-1.21
$FeOH_2^+$	0,0	0,0	0,0	0,0	1,1	0,0	0,0	0,0	0,0	0,0	0,0	0,0	0,0	6.00
$Fe(OH)_2^+$	0,0	0,0	0,0	0,0	1,1	0,0	0,0	0,0	0,0	0,0	0,0	0,0	0,0	10.7
$Fe(OH)_3$	0,0	0,0	0,0	0,0	1,1	0,0	0,0	0,0	0,0	0,0	0,0	0,0	0,0	11.1
INT	0,0	0,0	0,0	0,0	0,0	0,0	0,0	0,0	0,0	0,0	0,0	1,1	1,1	-3.06
As(III)-Sand	1,1	0,0	0,0	0,0	0,0	0,0	0,0	0,0	0,0	0,0	0,0	0,0	1,1	-2.68
Fe(II)-Sand	0,0	0,0	0,0	1,1	0,0	0,0	0,0	0,0	0,0	0,0	0,0	0,0	1,1	-2.68

Table S4 (continued). TICKET Input Tableau for Fe-Catalyzed Oxidation of As(III) in the Sediment Column. Based on information from Bisceglia et al. (10)

	As(III)	As(IV)	As(V)	Fe^{2+}	Fe^{3+}	precip	iprecip	Fe(IV)	O_2	O_2*-	H_2O_2	INT-OH	Sand	
Kinetic Reactions														k
A3	0,0	1,-1	0,1	0,0	0,0	0,0	0,0	0,0	1,-1	0,1	0,0	0,0	0,0	9.50E+13
B1	0,0	0,0	0,0	1,-1	0,1	0,0	0,0	0,0	1,-1	0,1	0,0	0,0	0,0	4.67E+07
B2	0,0	0,0	0,0	1,-1	0,1	0,0	0,0	0,0	0,0	1,-1	0,1	0,0	0,0	8.64E+11
F1	0,0	0,0	0,0	1,-1	0,0	0,0	0,0	0,0	0,0	0,0	1,-1	0,1	0,1	2.33E+06
F2	0,0	0,0	0,0	1,-1	0,0	0,0	0,0	0,0	0,0	0,0	1,-1	0,1	0,1	7.02E+10
I3	0,0	0,0	0,0	0,0	0,0	0,0	0,0	0,1	0,0	0,0	0,0	1,-1	1,-1	8.64E+10
J1	0,0	0,0	0,0	1,-1	0,2	0,0	0,0	1,-1	0,0	0,0	0,0	0,0	0,0	1.65E+08
J2	0,0	0,0	0,0	1,-1	0,2	0,0	0,0	1,-1	0,0	0,0	0,0	0,0	0,0	7.19E+11
J4	1,-1	0,1	0,0	0,0	0,1	0,0	0,0	1,-1	0,0	0,0	0,0	0,0	0,0	3.60E+10
R1	0,0	0,0	0,0	0,1	1,-1	0,0	0,0	0,0	0,1	1,-1	0,0	0,0	0,0	1.30E+13
R2	0,0	0,0	0,0	0,1	1,-1	0,0	0,0	0,0	0,1	1,-1	0,0	0,0	0,0	1.30E+19
R3	0,0	0,0	0,0	0,1	1,-1	0,0	0,0	0,0	0,1	1,-1	0,0	0,0	0,0	6.50E+23
P1	0,0	0,0	0,0	0,0	2,-2	0,1	0,1	0,0	0,0	0,0	0,0	0,0	0,0	2.67E+35
P2	0,0	0,0	0,0	0,0	1,-1	1,0	0,1	0,0	0,0	0,0	0,0	0,0	0,0	2.12E+24

Notes:

(a) All kinetic reaction rates (k) are given in M^{-1} day^{-1} or day^{-1}

(b) Reactions are identifed in Hug and Leupin (2003)

(c) Reaction rate coefficients are specified at pH = 8.3

(d) As(III)-Sand and Fe(II)-Sand equilbrium coefficients are assumed and correspond to 9:1 partitioning between sorbed and dissolved phases

(e) Sorption reactions for As(III) and As(V) onto iron oxides (as defined by Bisceglia et al. (2005)) were excluded from sensitivity calculations for simplicity